Austrian Journal of Earth Sciences | Volume 97 | 24 - 37 | Vienna | 2005

Geomorphic Response of Alluvial Rivers to Active Tectonics: Example from the Southern Rhinegraben

M. GIAMBONI*), A. WETZEL & B. SCHNEIDER

Geologisch-Paläontologisches Institut, Universität Basel, Bernoullistrasse 32, CH-4055 Basel
*) coresponding author (present address): Forstdirektion - Schutzwald und Naturgefahren Bundesamt für Umwelt, Wald und Landschaft CH-3003 Bern

KEYWORDS
morphometry
Neotectonics
alluvial rivers
Upper Rhinegraben

Abstract

The folding of a middle Pliocene marker horizon documents the tectonic deformation of the southern Rhinegraben during the Plio-Pleistocene. Morphometric analysis of drainage basins implies that tectonic activity is ongoing in the studied area, the Sundgau, where lithology and climate can be considered as uniform. Two kinds of geomorphic properties were analyzed: properties related to channel network geometries (stream gradient, drainage density, total stream length), and properties related to basin geometry (area, relief, slope, hypsometry). Significant correlations are found between tectonic uplift and channel network properties. Drainage basin parameters are only in part related to tectonic effects and seem to obey laws that are independent of uplift. The topographic record of tectonic activity strongly depends on the spatial scale of the observed basins: The most significant relationships between uplift and geomorphic variables have been observed in basins of intermediate size (5-10 km^2). Larger basins (>10 km^2) lack geomorphic properties of tectonic origin suggesting that they are able to quickly adjust to changes in base level. Geomorphic response of small basins (<5 km^2) is perturbed by local aging processes (e.g. microclimate, agriculture, land cover) and noise.

The results demonstrate that the southern Rhinegraben is affected by active tectonism, and that, secondly, the applied methods are useful tools for detecting ongoing deformation, even in regions of modest uplift rates (<0.1 mm/a).

Die tektonische Aktivität im südlichen Rheingraben während des Plio-Pleistozäns ist durch die Verfaltung eines mittelpliozänen Referenzhorizontes dokumentiert. Morphometrische Analysen von Einzugsgebieten zeigen, dass die tektonische Aktivität im Sundgau, dessen Lithologie und klimatische Verhältnisse als einheitlich betrachtet werden können, immer noch ablaufen. Es wurden zwei Gruppen von geomorphologischen Merkmalen untersucht, solche, die mit der Geometrie des Entwässerungsnetzes zusammenhängen (Gerinneneigung, Entwässerungsintensität und gesamte Gerinnelänge), und solche, die mit der Geometrie des Einzugsgebietes in Verbindung stehen (Fläche, Relief, Hangneigung, Hypsometrie). Es zeigt sich eine ausgeprägte Korrelation zwischen tektonischen Vertikalbewegungen und Merkmalen des Entwässerungsnetzes. Die Merkmale der Einzugsgebiete hingegen korrelieren nur teilweise mit tektonischen Bewegungen und scheinen anderen, nicht mit der Tektonik in Zusammenhang stehenden Einflüssen unterworfen zu sein. Die topographische Auswirkung tektonischer Aktivität ist stark von der Grösse der beobachteten Einzugsgebiete abhängig. Die wichtigste Korrelation zwischen Vertikalbewegung und geomorphologischen Variablen konnte in Einzugsgebieten mittlerer Grösse (5-10 km²) beobachtet werden. Die Merkmale von Einzugsgebieten grösser als 10 km² zeigen kaum Hinweise auf tektonische Bewegungen. Die geomorphologische Reaktion kleiner Einzugsgebiete (<5 km^2) auf tektonische Bewegungen wird hingegen stärker durch lokale Faktoren und Prozesse wie Mikroklima, landwirtschaftliche Nutzung, Variation in der Bodenbedeckung usw. beeinflusst.

Die Resultate zeigen (1) noch heute andauernde tektonische Aktivität im Gebiet des südlichen Rheingrabens und (2) die Eignung der eingesetzten Methoden, um aktive Tektonik auch in Gebieten mit kleinen Vertikalbewegungen (<0.1 mm/a) nachzuweisen.

1. Introduction

Relief results from interactions between climate, geologic parameters such as rock type and structure, and tectonically induced vertical crustal movements. Tectonism constructs landscapes through uplift and subsidence; climate affects the degradation of the landscapes by chemical and physical erosion (e.g. Ouchi, 1985; Keller, 1986; Keller and Pinter, 2002). Rock erodibility influences the efficiency of denudation processes (e.g. McKeown et al., 1988).

The aim of this study is to substantiate in an inductive way that the interplay between largely known tectonic processes and the resultant morphological features is ongoing.

The study area is situated at the southern end of the Rhinegraben and shows homogeneous climatic and geological settings. Neotectonic activity has been substantiated recently (Nivière and Winter, 2000; Laubscher, 2001; Meghraoui et al., 2001; Giamboni et al., 2004a; Giamboni et al., 2004b).

The relation between tectonics and morphologic response has been previously studied in strongly deforming areas, such as the Himalayas (e.g. Seeber and Gornitz, 1983; Hurtrez et al., 1999), California (e.g. Merritts and Vincent, 1989; Lifton and Chase, 1992), and Taiwan (Willemin and Knuepfer, 1994). However, there have been no attempts to systematically investigate geomorphic response to tectonism in areas with humid-temperate climate, smooth relief, and moderate tectonic activity such as the central European southern Rhinegraben (uplift rates < 0.1 mm/a: Müller et al., 2001; Giamboni et al., 2004b). The presented study shows that tectonic activity has a significant impact on geomorphologic properties, even if the deformation

rates are modest. The selected test area allows investigating this relationship because climate and lithological properties are essentially homogeneous throughout the area.

2. Physiographic and geologic settings

The study area is situated in the southernmost part of the Rhinegraben which is bounded in the south, southeast, and southwest by the Tabular Jura and the Jura Mountains, in the northwest by the Vosges, and in the north by the Alsacian plane (Fig. 1). This area, named Sundgau, is characterized by a hilly landscape with altitudes decreasing from south (400-450 m) to north (250-300 m). The relief flattens abruptly at the latitude of Mulhouse along a NE-SW trending continuous scarp between Dannemarie and Mulhouse (Fig. 1). The Rhine River represents the eastern boundary of the Sundgau (Fig. 1).

Present-day drainage system. The southern Rhinegraben comprises two main drainage basins separated by a NNW-SSE trending first-order watershed boundary (Fig. 1). The western basin drains south-westwards via the Doubs valley into the Bressegraben and belongs to the Mediterranean catchment area. The eastern basin is that of the Rhine river, including the subbasin of the Ill river (eastern Sundgau area), and forms part of the North Sea drainage basin (Fig. 1).

The western basin is dewatering in the southern part through three main tributaries (Allaine, Coeuvatte, and Vendline), all of which rise in the northern Tabular Jura (Ajoie). In the north and northeast, the tributaries of the Doubs river are the Savoureuse rising in the Vosges Mountains, and the Bourbeuse together with its main tributary Suarcine (Fig. 1).

The eastern area comprises two main drainage subbasins, separated by a 2nd order water divide: the Ill River with the main tributary reaches Largue and Thalbach in the south and the Doller in the north, and the drainage system of the Rhine valley (Fig. 1).

In their upper course, the Ill and Largue rivers flow in the Mesozoic sediments of the Ferrette anticline. The rest of the courses are situated in the Rhinegraben. The Thalbach River rises in the eastern part of Sundgau area and flows exclusively within the Rhinegraben. In the northern part, the Doller River is the main affluent of the Ill drainage basin. It originates in the southern Vosges, flows in the upper part ESE and changes its direction to the NE when it reaches the Alsacian plain. The confluence with the Ill River is north of the city of Mulhouse (Fig. 1).

The investigated drainage basins are entirely situated within the Sundgau area (Fig. 1), i.e., within the Rhinegraben, and show similar geological, topographical and climatic conditions.

Geology. The Tertiary fill of the southern Rhinegraben mainly consists of a marine to brackish Oligocene substratum and a terrestrial Plio-Pleistocene cover. Except in the southern-most part of Sundgau where Early Oligocene sandstones dominate, Late Oligocene marls, mainly marine marls, constitute the bedrock of the Plio-Pleistocene clastics (Théobald and Dubois, 1958; Ruhland and Blanat, 1973). The Pliocene gravels and sands are called Sundgau gravel. They are overlain by up to 20 m thick Würmian loess (Liniger, 1967).

Climate. The climate is characterized by temperate winters with amounts of precipitation of about 150 mm and average temperatures of 0°-2° C, and by humid summers with total precipitation of 250-300mm and average temperatures of 20°-25° C. The distribution of the annual net precipitation shows a regional decrease from the Jura mountains in the south (about 1000 mm) to the Alsacian plane in the north (about 800 mm). During the Pleistocene glacial periods, the study area was situated in the northern foreland of the glaciers which covered parts of the Jura Mountains. Therefore, in the study area crystic activity couldn't be observed.

3. Plio-Pleistocene tectonic activity

The Sundgau gravel. The youngest sediment encountered in the area – apart from the Quaternary loess cover and the alluvial valley fills – is the Sundgau gravel of Middle Pliocene age (4.2 to 2.9 Ma: Petit et al., 1996).

The Sundgau gravel consists of up to 70% Alpine and Molassic coarse material (Liniger, 1967) and was deposited by a precursor of the present-day Rhine river, which flowed at that time from the Alps through the southern part of the Rhinegraben towards the west to reach the Bressegraben southwest of Besançon (e.g. Liniger, 1966; Villinger, 1998). Later, during Piacenzian and Quaternary times, uplift in the Bressegraben (Sissingh, 1998) and subsidence in the Rhinegraben (e.g. Doebl, 1970; Schumacher, 2002) led to the deviation of this paleo-River, initiating its present-day flow towards the north into the Rhinegraben (Liniger, 1966; Petit et al., 1996; Giamboni et al., 2004b).

The Sundgau gravel was deposited by a shallow braided river, providing a shifting network of unstable, low-sinuosity channels. Depth of the channels is on the order of 1 m (e.g. Liniger, 1967;

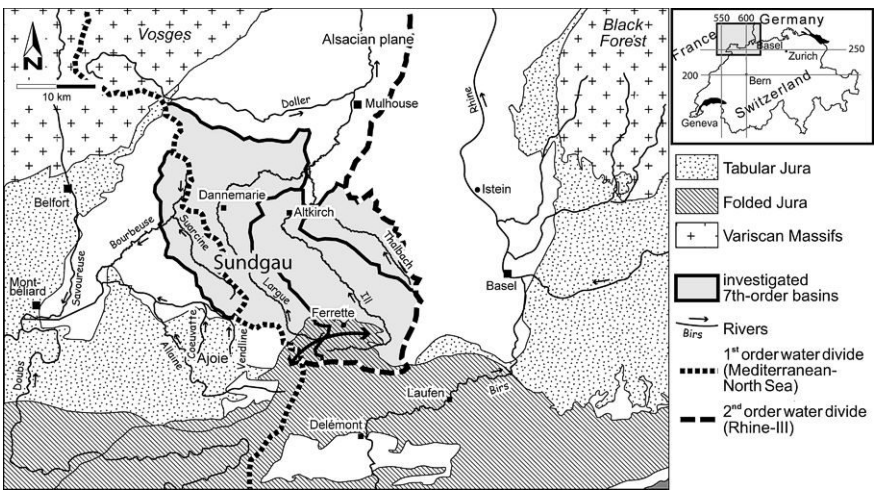

Figure 1: Simplified structural map of the study area with major hydrographical and geological characteristics.

Giamboni et al., 2004a). The channels are preserved as tabular bodies exhibiting numerous minor internal erosional surfaces. The gravel is up to 30 m thick.

These sedimentological characteristics indicate that the base of the Sundgau gravel formation accumulated on a semi-planar and horizontal surface. This planar surface represents an ideal marker horizon for resolving post Middle Pliocene differential vertical displacements due to folding and faulting.

The Sundgau gravel is exposed within an E-W striking 20 km wide belt, between the Rhine River and the entrance to the Doubs valley near Montbéliard (Fig. 1). The eastern parts of the Sundgau gravel were eroded by the Rhine River. Downstream, in the Doubs valley, several alluvial terraces of the Sundgau gravel system are preserved (Contini et al., 1973). Towards the south, the Sundgau gravel covers the northernmost part of Tabular Jura (Fig. 2). North of the latitude of Dannemarie-Altkirch, the Sundgau gravel interfingers with the Pliocene gravel and sands shed by paleo-rivers draining the Vosges mountains (Théobald and Devantoy, 1963; Ménillet et al., 1989).

Deformation marker. Today the Sundgau gravel marker horizon is deformed by more than ten narrow and laterally plunging, predominantly SW-NE striking folds (Fig. 2: Giamboni et al., 2004a). The fold amplitudes are nearly conformable to topographic structures and, thus, suggest very young tectonism. The fold amplitudes are highest in the south, at the boundary between the Rhinegraben and the adjacent Tabular Jura (Giamboni et al., 2004a). The upfolding of the Sundgau gravel is spatially related to late Paleozoic structures on the basement and it appears that these structures became transpressively reactivated (Ustaszewski et al., 2001; Giamboni et al., 2004a).

The described deformation is ongoing, as shown by recent studies on river and valley morphology revealing tectonic activity up to Pleistocene (Nivière and Winter 2000; Giamboni et al. 2004b).

4. Methodological Approach

To semi-quantitatively describe the interplay between uplift and erosion, and to identify the response of the drainage basin morphologies, selected geomorphic indices are used as basic reconnaissance tools. The results are then combined with geological data about the spatial distribution of crustal movements to test the methods and to produce a thorough assessment of the relative degree of activity in the area.

Two categories of variables were investigated: variables related to shape and channel network of rivers (stream gradient index and stream slope, that is, longitudinal profiles; stream length, drainage density), and variables associated with the morphology of drainage basins (e.g., area, hypsometric integral, relief, and slope).

4.1. River characteristics and channel networks

Conceptual model of equilibrium and the stream gradient index (SL). According to the theory of “graded streams”, the longitudinal profile of a river sensitively responds to uplift (Mackin, 1948): a stream not subjected to base-level change eventually reaches a stable longitudinal form that reflects no net erosion or deposition and is "at grade”. With falling base level, the stream tends to maintain a steady longitudinal shape by uniform incision. In both situations, the equilibrium, or steady form, results from the interactions of stream power, sediment transport, and bed gradient (Gilbert, 1877). The potential ability of a stream reach to react to downstream base-level changes depends upon the delivery of water and sediment from upstream and on local settings. Therefore, non-equilibrium mainly results from three factors: low erodibility of the bedrock (McKeown et al., 1988), local base level changes due to tectonics or sea level fluctuations (Seeber and Gornitz, 1983; Bull and Knuepfer, 1987; McKeown et al., 1988; Zuchiewicz, 1995), and changes in water discharge and sediment load, due to climatic changes or tributary junctions (Galay, 1983).

For drainage basins in equilibrium stage, the gradient of rivers decreases downstream as the discharge increases. Their profile can be expressed by a straight line in a semi-logarithmic plot (Hack, 1973):

$$H = C - k \cdot \ln L \qquad (1)$$

where H is the altitude at a given point in the profile, L the distance

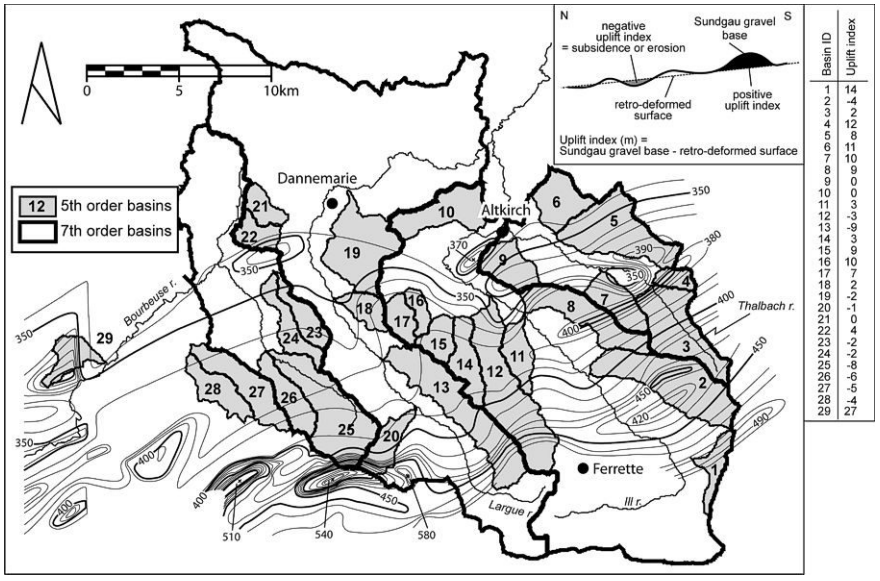

Figure 2: Base map of the Pliocene Sundgau gravel (isohypse units in meters above sea level). This marker horizon is deformed by several narrow and laterally plunging predominantly SW-NE striking folds. Present-day major rivers and investigated 7th- and 5th-order basins are superimposed. Inset: sketch showing the method used to infer the uplift index by retrodeforming the folded base of the Sundgau gravel. Uplift index values for the 5th-order basins are drawn on the right (in m).

from the source, C is a constant, and k is the slope of the straight line. The slope S of the stream at a given point is the derivate of this equation with respect to L and, hence, is defined as

$$S = \frac{\Delta H}{\Delta L} = \frac{\Delta(C - k \cdot \ln L)}{\Delta L} = \frac{k}{L} \quad (2)$$

It follows that k = SL, where SL is the stream-gradient index (Hack, 1957; 1973). SL is simply the product of the channel slope at a given point and the channel length to the source, and it equals

$$SL = \frac{\Delta H}{\Delta L} \cdot L \quad (3)$$

where ?H is the difference in elevation between the ends of the reach of interest, ?L is the length of the reach of interest, and L the distance of the reach from the source.

SL correlates to stream power. Total stream power available at a particular reach of channel reflects the ability of a stream to erode its bed and transport sediment. Total or available stream power is proportional to the slope of the channel bed, and there is a good correlation between total channel length upstream and bankful discharge, which is thought to be important in forming and maintaining rivers. However, the gradient index values reflect spatial variations in discharge, but usually it is the result of lithologic or tectonic controlled reaches of a river (e.g. Seeber and Gornitz, 1983; McKeown et al., 1988; Bul, 1990). Schumm (1986) considered the longitudinal profile of streams even one of the most sensitive indicators of slope change.

In ideal cases - i.e. for rivers “at grade” – longitudinal profiles describe a concave shape with gently decreasing slopes and homogeneous SL values.

In this study, the longitudinal river profiles are obtained from 1:25'000 French topographic maps. The distance along the river channel between consecutive contours crossing (5 to 2.5 m intervals) is measured. The origin of the profile is at the source of the river. The river profile is plotted in a graph with axis in Euclidian distances together with the SL values for several reaches of interest (Fig. 3).

Sinuosity index (SI). Sinuosity is the ratio between channel length (l) and valley length (L) and it is also the ratio between valley slope (S_v) and channel gradient (S):

$$SI = \frac{l}{L} = \frac{S_v}{S} \quad (4)$$

Experimental studies as well as field observations (Schumm, 1981; 1993) have demonstrated that much of the sinuosity variability of alluvial rivers reflects the variability of the valley slope. Thus, changes of valley-floor slope provide an explanation of downstream changes of sinuosity. Tectonic activity can be one of the forces controlling the changes of valley floor slope, together with local changes of sediment and water supply due to river junctions or changes in lithology (e.g. Schumm, 1986).

Drainage density. Drainage density is defined as the sum of all channel lengths divided by the drained area (Horton, 1932). Channel lengths as well as drainage areas were extracted from DEM data.

Drainage density is recognized as an indicator for the intensity of fluvial erosional processes and reflect topographic, lithological, and climate controls.

4.2. Drainage basin morphology

The drainage basins were extracted from the available DEM according to the stream ordering of Horton (1945). Basins of 1st

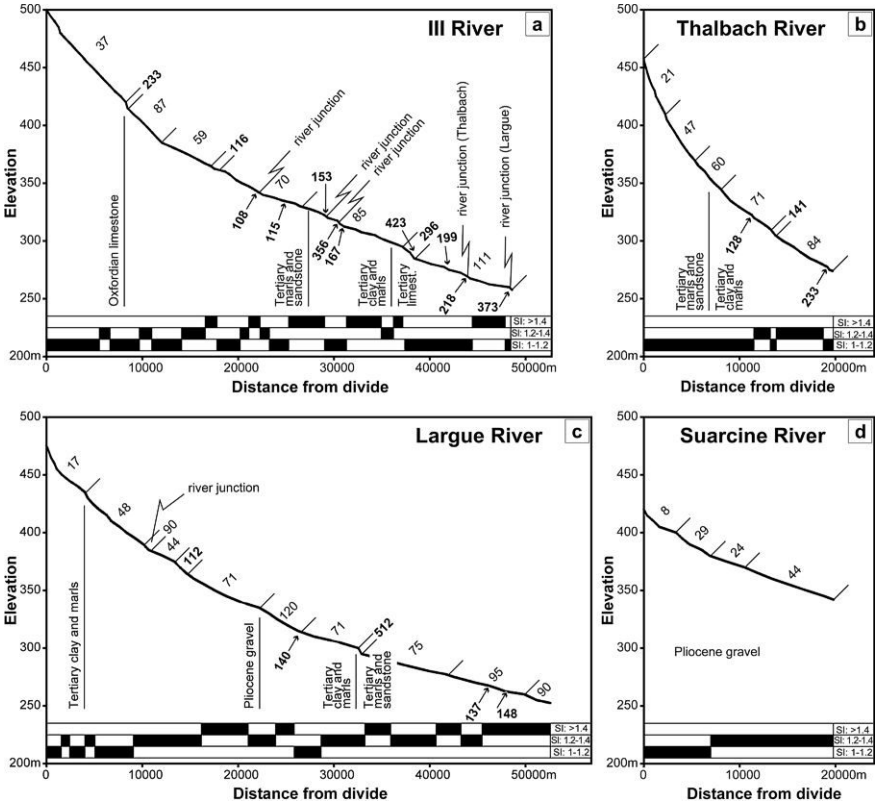

Figure 3: Longitudinal profiles of the Ill (3a), Thalbach (3b), Largue (3c) and Suarcine (3d) rivers. Stream gradient index (SL) values are shown to the right of each segment. Anomalously high SL values for individual reaches are indicated by arrows and/or bold characters. Lithologic changes in the river bed are specified by vertical bars beneath the profile. Stream junctions of the main branch with tributaries are marked above the profile. Sinuosity changes in sinuosity index classes are plotted on the bottom of each profile. Sinuosity Index (SI): *1-1.2* = straight to low sinuosity; *1.2-1.4* = moderate sinuosity; *>1.4* = high sinuosity.

and 2nd order are highly sensitive to local settings (Vergnes and Souriau, 1993) such as micro-climate, exposition, and anthropogenic influences, and, thus, were not considered. The investigated variables were calculated for basins of 3rd, 4th and 5th order, which are considered reliable for detecting tectonic activity (e.g. Merritts and Vincent, 1989; Merritts et al., 1994). 5th order basins were used for the analysis of tectonic activity, and basins of 7th and higher order were analyzed for the regional synthesis (Fig. 2 and Tab. 2).

Basin area, relief, and slope. Basin relief is the elevation difference between the highest and the lowest point in the drainage basin (Ohmori, 1993). All three variables are calculated from the available DEM.

Hypsometric curve and hypsometric integral. The hypsometric curve describes the distribution of elevations within an area of land, in this case within singular drainage basins. The basin contours as well as the hypsometric data were calculated from the DEM. The hypsometric curve is defined as:

$$x = f_{(y)} \quad (5)$$

where

$$x = \frac{a}{A}$$

A = total surface area of the basin, i.e., the number of DEM cells
a = surface area within the basin above a given elevation

$$y = \frac{h}{H}$$

H = total relief of the basin (= $H_{max} - H_{min}$)
h = elevation of a given cell in the DEM

Because of the normalized height and area values, the hypsometric curve is independent of absolute basin size and relief.

To characterize the shape of the hypsometric curve for a given drainage basin, its hypsometric integral (Hi) was calculated according to Strahler (1952):

$$Hi = \int_{\min elevation}^{\max elevation} \frac{a}{A} \cdot \Delta\left(\frac{h}{H}\right) \quad (6)$$

Strahler (1952) applied this technique to several drainage basins in areas of diverse relief, climate, geology, rock resistances and vegetation, but in essentially tectonically inactive regions. He found that the hypsometric integral was inversely correlated with drainage basin relief, slope and channel gradient. Merritts and Vincent (1989) correlated these parameters with rates of vertical tectonism. They conclude that in areas with uniform climate, geology, and vegetation, the hypsometric integral correlates inversely to vertical tectonic activity.

Strahler's theoretical evolution of landscapes distinguishes between three main stages: a "youthful, non-equilibrium" stage (Hi = 0.6 to 1.0), a "mature equilibrium" stage (0.35 to 0.6), and an "old age" (0.0 to 0.35). This classification was later questioned by Ohmori (1993). He showed that in areas with concurrent tectonics and denudation, such as in the Japanese mountains, the results of the hypsometric integral are reverse of Strahler's theory.

In the presented study drainage basins are classified by the shape of the hypsometric curve (convex, concave, s-shaped or nearly linear), by the absolute distribution of the elevations (homogeneous, skewed, bimodal) and by the hypsometric integral (Fig. 6).

4.3. Uplift index and multivariate correlation analysis

Uplift indices were obtained by combining the base map of the Pliocene series (Sundgau gravel, Fig. 2) as a marker for the post 3Ma deformation, with a surface that decreases gently towards the north approximating the paleo-base of the Pliocene (index horizon). The latter surface was obtained by retrodeforming the single folds at the base of the Pliocene sediments (see inset of Fig. 2). The elevation difference between the two surfaces was calculated. Regional tilting was not taken into account. The absolute values are used as the indexing variable in Tab. 2. Because of the uncertain time constrain for folding, uplift rates were not calculated.

The morphometric variables and the uplift indices were used to extract a variable highly correlative to uplift rate (Pearson correlation coefficient; Tab. 1).

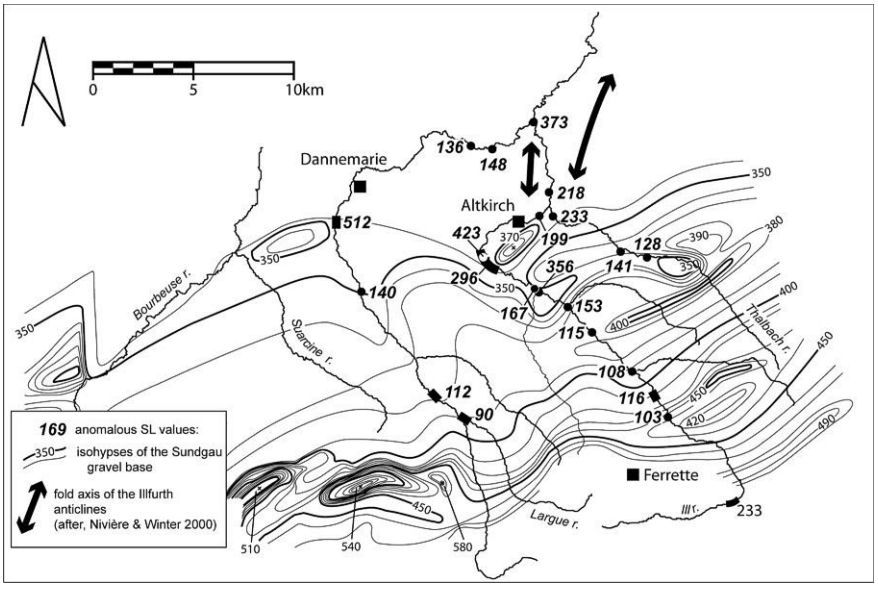

Figure 4: Map of anomalously high SL values and isohypses of the Sundgau gravel base.

5. Geomorphic Response to Tectonism

5.1. Stream gradient index

The stream profiles of four main rivers were used to evaluate the tectonic activity in the test area. The Thalbach, the Ill and the Largue rivers belong to the Rhine river catchment and intersect several folds (Fig. 3a-c), whereas the Suarcine river (Fig. 3d) is a tributary of the Doubs and flows in a tectonically nearly undeformed area (Fig. 4). The Thalbach and Suarcine rivers are small and differ in the tectonic setting. The other rivers have larger catchment areas and are expected to differ in the tectonically controlled alluvial dynamic.

Reaches with constant or nearly constant SL values are designated as segments and are delimited by oblique bars in the plots (Fig. 3).

Ill River. The uppermost course of the Ill River flows completely within Mesozoic sediments of the Ferrette Anticline (Fig. 1) and shows a constant decreasing channel gradient with SL values of 37 (Fig. 3a). Sinuosity of 1-1.2 indicates straight channels. The transition from the Jura Mountains into the Rhinegraben is marked by a short but steep reach (SL = 233, Figs. 3b, 4).

The middle course (km10 to km 35) is characterized by moderate SL values ranging from 59 to 87. Four zones of anomalously high SL values were identified (Figs. 3a, 4). The first one (SL = 116) is located in the prolongation of a fold observed in the Sundgau gravel base map (Fig. 4). The second (SL = 108) coincides with the junction of the Ill river with one of its major tributaries (Fig. 4). Further downstream, a zone of remarkably high SL is situated near the junction with the second main tributary river and at the interference with the southwestern limb of the Altkirch anticline (SL = 153, 356, 167) (Fig. 4).

The lower part of the Ill river is first characterized by a segment with the highest SL value encountered (423) corresponding to the reach flowing around the northwestern nose of the Altkirch anticline (Fig. 4). Further down, the Ill river entrenches the Illfurth anticline (Fig. 4) and flows in a S-N trending gorge (Nivière and Winter, 2000; Giamboni et al., 2004b). The channel gradients are generally high (SL = 111), with peaks at 199 and 218.

The Ill river is characterized by straight to lowly sinuous channels (SI = 1-1.2) in the upper course and a gradual transition to moderately (SI = 1.2-1.4) and highly (SI = >1.4) sinuous channels in the middle part (Fig. 3a). The lower course is subdivided into a straight to lowly sinuous channel along the Illfurth gorge and a high-sinuosity reach further downstream.

Thalbach River. The river profile shows a strong gradient with a general increase of SL values from 21 to 84 (Figs. 3b, 4), disturbed by two high SL values (128, 141). In the middle course, the channel changes from lowly to moderately sinuous.

Largue River. The Largue river has a number of segments with alternating high and low SL values ranging from 17 to 120 (Fig. 3c). In general, the upper part has low average values around 45, the middle part moderate (around 70), and the lower part higher average values (around 90).

Reaches with anomalously high SL values occur (1) at the transition from upper to middle course (SL=112), (2) at the junction with a tributary (SL=140), and (3) at the transition from the middle to the lower river course (SL=512) where the lithology changes from clay to marls (Fig. 4). Other anomalies (137, 148) were encountered in the lowermost part of the Largue River.

The river course changes from straight/low sinuous channels in the upper valley to moderately/highly sinuous channels in the middle and lower valley (Fig. 3c).

Suarcine River. The river shows a gently decreasing gradient to the mouth and moderate increasing SL values. No anomalously high SL values occur. The river course changes from straight/lowly sinuous in the upper part to moderately sinuous in the lower part (Fig. 3d).

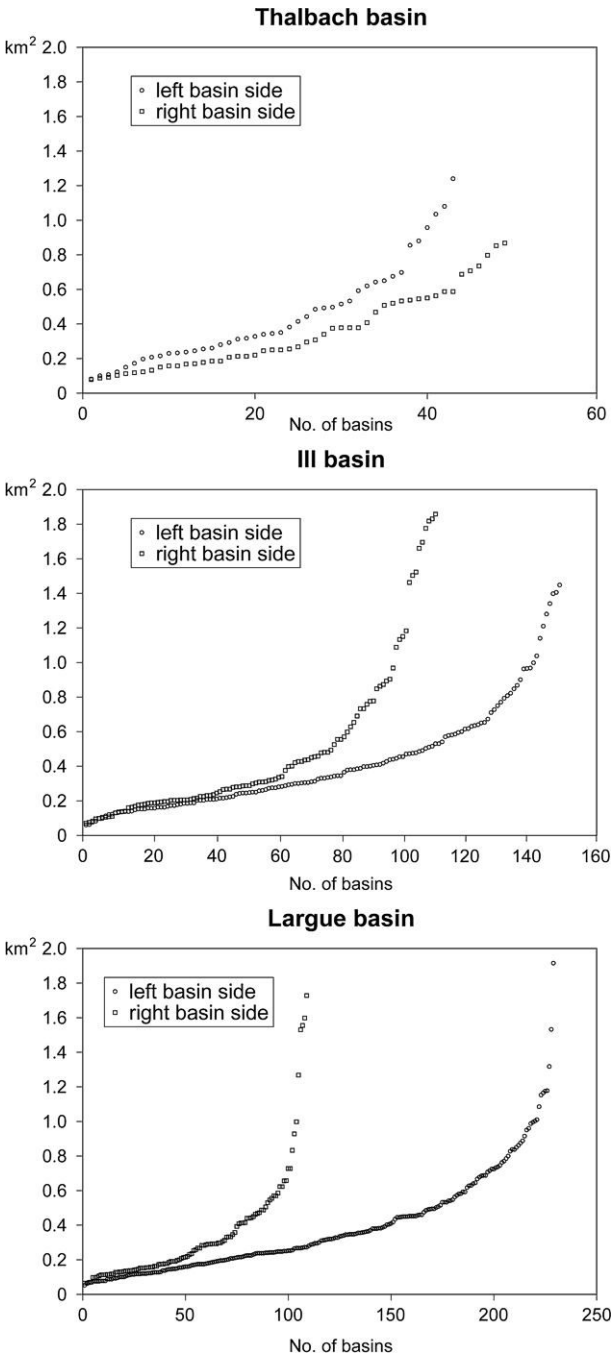

Figure 5: Area distribution of 3rd-order basins situated within the 7th-order basins of the Thalbach, Ill, Largue and Suarcine rivers. Left and right 7th-order basin sides are plotted separately.

Synthesis. The presented data evince a multitude of anomalies that may result from changes in lithology, form changes in discharge at river junctions, and from tectonic uplift.

The stream-gradient index SL is useful for documenting changes in lithology, if the resistance of the eroded rocks is clearly different (e.g. McKeown et al., 1988). This is the case at the transition from Oxfordian limestones to Tertiary marls along the Ill river profile (Fig. 3a; SL = 233), as well as at the transitions from Pliocene gravels to Tertiary clays (from SL 71 to SL 120) and from Tertiary clays to marls (512), along the Largue river profile (Fig. 3c). A clear correlation between the lithology and the changes in sinuosity, however, could not be observed.

High SL values can also result from discharge growth caused by the junction of the main river with its tributaries. This effect - observable only along the two large rivers Ill and Largue - is characterized in the river profile by a knick point with high SL values followed by gentle gradients with moderate SL (Ill river: SL 108, 153, 356, 218, 373; Largue river: SL 90, 140).

The relation between SL indices and tectonic deformation is threefold: (1) Local anomalies of the SL values are clearly related to discrete tectonic structures (folds observed at the base of the Sundgau gravel; Fig. 2), and are not influenced by other factors such as lithology or discharge growth. Related anomalies occur along the Ill River (SL 116, 115, 296, 423) and along the Thalbach River (SL 128, 141). (2) SL values are partly a result of a lithology or discharge change, but the anomalously high values are emphasized by discrete uplift. Such reaches are found along the Ill river (SL 356 at the junction point with a tributary) and along the Largue river (SL 512, at the transition from Oligocene clay to Oligocene marls and sandstone). (3) SL values of the different drainage basins are generally different. For instance, the average SL values between the Ill river (average SL 37-111) differs from the SL values of the Largue river (average SL 15-95), the latter being less affected by uplift deformation (Fig. 4). A more pronounced difference is observed when comparing the small basin of the Thalbach (average SL 21-85) and the Suarcine river (average SL 8-44), the latter being situated in an area of very small vertical movement (Fig. 4).

Furthermore, increased sinuosity indices due to the lowering of slope produced by the rising anticlines are characteristic (Fig. 4). Detailed Studies on fluvial morphology confirm these observations with similar results on sinuosity and a radical change on sedimentation from accumulation uphill from the anticlines, to erosion with coarse bed layers over the anticline (L. Schmitt, pers. Comm.).

5.2. Linear correlation analysis (Pearson)

Possible correlations between morphometric parameters and uplift indices were evaluated by means of a Pearson linear correlation analysis (e.g. Merritts and Vincent, 1989; Summerfield and Hulton, 1994; Hurtrez et al., 1999). The analyzed variables were: basin area, total stream length, average basin slope, basin relief, hypsometric integral, and drainage density. All variables are calculated for the 5th order basins and their 4th- and 3rd-order subbasins (Tabs. 1, 2). Significance of each correlation was determined by a t-test with the 5% level of significance. Hence, correlation coefficients greater than 0.38 were considered significant.

The results of the correlation analysis (Tab. 1) indicate that only few morphometric parameters correlate to uplift index. Drainage density shows a moderate negative correlation with uplift index for all basin orders (coefficient [*r*] -0.383 to -0.472). The most significant correlations are observed between basin area and morphometric variables characterizing the drainage network, such as drainage density, total stream length, basin slope, and basin relief. The frequency of these correlations increases with decreasing basin order (Tab. 1). Conversely, correlation of drainage density with hypsometric integral, basin relief, and basin slope decreases with decreasing basin order.

These findings suggest that (1) drainage network properties (drainage density and total stream length) are directly related to the

	Uplift index	Area xth	Tot str. leng. xth	Drain. d. xth	Hyp. int. xth	B. relief xth	B. slope xth
Uplift index	1						
Area, 5th	**-0.469**	1					
Tot stream length, 5th	**-0.519**	**0.981**	1				
Drain. dens., 5th	**-0.383**	-0.063	0.097	1			
Hyps. integr., 5th	-0.205	-0.230	-0.181	**0.414**	1		
Basin relief, 5th	0.061	**0.644**	**0.526**	**-0.582**	-0.244	1	
Basin slope, 5th	0.285	0.150	0.029	**-0.677**	-0.311	**0.640**	1
Uplift index	1						
Area, 4th	-0.364	1					
Tot stream length, 4th	-0.227	0.272	1				
Drain. dens., 4th	**-0.441**	**0.824**	**0.735**	1			
Hyps. integr., 4th	-0.263	0.299	0.167	0.354	1		
Basin relief, 4th	-0.285	**0.851**	0.249	**0.706**	0.322	1	
Basin slope, 4th	-0.077	**0.740**	0.188	**0.572**	0.119	**0.756**	1
Uplift index	1						
Area, 3th	-0.131	1					
Tot stream length, 3th	**-0.470**	**0.387**	1				
Drain. dens., 3th	**-0.472**	**0.526**	0.187	1			
Hyps. integr., 3th	0.196	**-0.533**	**-0.710**	-0.348	1		
Basin relief, 3th	-0.035	**-0.582**	-0.239	-0.344	**0.578**	1	
Basin slope, 3th	-0.145	0.044	0.085	0.093	-0.049	0.065	1

Table 1: Pearson linear correlation matrix for geomorphic variables and the uplift index for 5th-order basins and their 4th- and 3rd-order subbasins. (*) Values with correlations significant at 95% confidential level.

		Thalbach						III									
5th order basin ID		3	4	5	6	7	9	1	2	8	10	11	12	14	15	16	17
No. Basins	5th order-basin	1	1	1	1	1	1	1	1	1	1	1	1	1	1	1	1
Area (km²)		15.40	2.70	17.40	7.93	7.14	7.07	4.76	20.34	11.97	10.27	5.73	21.21	6.88	4.46	2.66	4.09
Tot stream length (km)		149.02	21.00	163.36	69.82	65.49	64.37	36.69	158.31	106.65	91.44	52.96	204.06	68.38	45.66	28.17	42.83
Drainage density (km/km²)		9.68	7.79	9.39	8.80	9.18	9.10	7.70	7.78	8.91	8.90	9.25	9.62	9.93	10.23	10.59	10.48
Hypsometric Integral		0.53	0.68	0.54	0.35	0.59	0.64	0.31	0.56	0.64	0.38	0.69	0.31	0.69	0.71	0.68	0.72
Relief (m)		126.00	70.00	115.00	94.00	120.00	116.00	129.00	171.00	127.00	95.00	104.00	162.00	88.00	75.00	64.00	66.00
Relief, S (m)		26.19	13.64	28.71	22.21	30.32	27.60	30.19	36.05	28.12	17.10	19.85	31.73	17.13	16.33	12.82	14.86
Slope (°)		2.38	2.08	2.42	2.77	2.66	3.77	2.85	2.88	2.34	3.40	1.95	3.11	2.21	2.46	2.22	2.06
Slope, S (°)		1.27	1.14	1.17	1.56	1.45	1.80	3.21	1.90	1.83	2.14	1.35	2.99	1.75	1.58	1.48	1.27
No. Basins	4th order-subbasins	2	2	4	4	3	3	2	3	3	3	2	6	3	2	2	2
Area, mean (km²)		4.61	0.94	2.72	0.95	1.72	1.85	2.15	3.22	0.90	2.48	1.80	2.13	1.87	1.13	0.63	1.81
Area, range (km²)		2.0-7.2	0.8-1.1	0.8-6.2	0.4-1.3	1.1-2.8	0.9-3.4	2.15-2.16	0.7-7.2	0.5-1.3	0.5-5.6	1.3-2.2	0.6-6.3	0.5-3.3	1.0-1.2	0.3-0.9	1.3-2.3
Tot stream length (km)		82.84	14.31	98.03	34.15	45.38	50.01	31.89	88.40	32.92	61.53	36.76	129.29	58.82	24.52	15.43	39.09
Drainage density, mean (km/km²)		8.79	7.58	9.35	9.19	8.85	8.32	7.41	9.04	9.02	8.76	10.22	10.42	9.96	10.85	12.26	11.01
Drainage density, S (km/km²)		0.47	0.21	0.63	1.23	0.77	1.45	0.75	0.16	0.95	0.68	0.00	1.03	1.14	0.46	0.09	0.94
Hypsometric Integral, min		0.49	0.68	0.33	0.30	0.41	0.63	0.43	0.44	0.41	0.33	0.26	0.16	0.68	0.72	0.53	0.69
Hypsometric Integral, max		0.68	0.70	0.70	0.58	0.68	0.70	0.44	0.64	0.66	0.53	0.65	0.76	0.77	0.73	0.56	0.74
Hypsometric Integral, mean		0.56	0.69	0.59	0.37	0.64	0.67	0.43	0.55	0.53	0.42	0.63	0.41	0.71	0.72	0.55	0.71
Hypsometric Integral, S		0.06	0.01	0.08	0.10	0.05	0.03	0.00	0.04	0.11	0.03	0.05	0.22	0.03	0.00	0.01	0.03
Relief, mean (m)		84.50	39.00	58.50	67.25	81.67	86.33	86.50	66.33	24.75	67.33	53.50	52.25	48.00	43.50	21.00	51.50
Relief, S (m)		17.69	7.07	33.47	14.86	5.13	15.95	48.79	45.00	18.43	16.20	4.95	21.84	7.81	0.71	1.41	0.71
Slope, mean (°)		2.04	1.67	1.95	3.03	2.38	3.63	2.99	1.50	1.11	3.84	1.56	2.23	1.98	1.93	1.41	1.84
Slope, S (°)		0.33	0.01	0.52	0.54	0.19	0.32	1.37	0.47	0.43	1.72	0.23	1.01	0.46	0.17	0.14	0.00
No. Basins	3rd order-subbasins	14	5	23	11	9	11	3	15	13	11	5	22	12	6	6	4
Area, mean (km²)		0.51	0.45	0.40	0.31	0.23	0.49	0.79	0.31	0.44	0.52	0.38	0.52	0.37	0.18	0.35	0.40
Area, range (km²)		0.2-1.5	0.1-1.1	0.1-1.3	0.1-0.6	0.1-0.5	0.1-1.5	0.2-1.8	0.1-0.8	0.1-0.9	0.1-1.4	0.1-0.6	0.1-1.5	0.1-1.5	0.1-0.3	0.1-0.7	0.2-0.7
Tot stream length (km)		82.46	9.60	85.10	34.99	29.73	33.36	26.80	62.44	44.23	52.00	17.29	87.47	34.08	30.94	13.05	32.75
Drainage density, mean (km/km²)		10.45	7.84	8.90	10.24	9.33	9.37	6.66	10.34	10.28	10.13	10.45	11.82	10.35	10.20	10.27	10.05
Drainage density, S (km/km²)		2.75	2.28	2.29	2.02	2.48	1.71	0.61	1.91	1.77	3.08	3.21	2.00	3.92	2.23	2.28	2.53
Hypsometric Integral, min		0.45	0.45	0.28	0.30	0.39	0.32	0.38	0.42	0.38	0.39	0.53	0.14	0.42	0.56	0.52	0.65
Hypsometric Integral, max		0.72	0.72	0.72	0.68	0.74	0.71	0.45	0.75	0.74	0.61	0.75	0.78	0.71	0.72	0.68	0.73
Hypsometric Integral, mean		0.63	0.58	0.56	0.44	0.62	0.65	0.42	0.59	0.57	0.45	0.66	0.50	0.62	0.66	0.61	0.69
Hypsometric Integral, S		0.07	0.07	0.11	0.11	0.09	0.07	0.04	0.11	0.12	0.07	0.08	0.17	0.07	0.05	0.07	0.03
Relief, mean (m)		50.79	15.4	38.57	49.7	42.11	54.55	67.33	42.53	17.92	56.18	16.40	24.22	15.80	32.50	19.00	29.00
Relief, S (m)		15.64	4.83	18.38	21.77	16.82	12.60	40.46	15.73	12.57	20.67	11.15	14.69	6.78	11.47	10.51	10.61
Slope, mean (°)		2.20	1.49	2.25	2.82	2.21	3.59	3.10	2.55	1.18	4.16	1.25	2.55	1.45	1.89	1.70	1.56
Slope, S (°)		0.57	0.39	0.76	0.75	0.75	0.78	1.31	1.64	0.41	1.74	0.25	2.37	0.40	0.55	0.47	0.39
Uplift, mean (m)		**2**	**12**	**8**	**11**	**10**	**0**	**14**	**-4**	**9**	**0**	**3**	**-3**	**3**	**9**	**10**	**7**
Uplift, S (m)		**7.17**	**11.79**	**10.02**	**0.19**	**10.97**	**2.53**	**5.93**	**8.56**	**9.61**	**0.2**	**5.72**	**5.86**	**6.91**	**2.23**	**1.17**	**2.13**
Uplift, max (m)		**31**	**31**	**30**	**18**	**32**	**6**	**20**	**17**	**27**	**0**	**16**	**10**	**13**	**13**	**13**	**11**

Table 2: Morphometric properties of 5th-order basins and their 4th- and 3rd-order subbasins (average values). Basins are arranged by their geographical location.

		Largue						Bourbeuse						
5th order basin ID		13	18	19	20	21	22	23	24	25	26	27	28	29
No. Basins	5th order-basin	1	1	1	1	1	1	1	1	1	1	1	1	1
Area (km²)		20.80	4.54	16.49	5.77	3.88	4.27	5.53	6.34	19.76	6.86	10.48	6.58	4.91
Tot stream length (km)		196.04	45.72	141.53	56.81	31.96	36.64	63.22	71.69	217.24	72.75	118.98	68.95	35.02
Drainage density (km/km²)		9.42	10.06	8.59	9.85	8.24	8.58	11.44	11.31	11.00	10.61	11.36	10.48	7.13
Hypsometric Integral		0.28	0.69	0.40	0.45	0.54	0.46	0.57	0.55	0.32	0.59	0.63	0.68	0.35
Relief (m)		128.00	78.00	110.00	64.00	60.00	76.00	47.00	52.00	71.00	47.00	56.00	47.00	85.00
Relief, S (m)		20.79	18.01	26.32	10.69	8.59	15.30	9.67	11.69	12.95	10.64	10.52	7.81	15.85
Slope (°)		2.66	2.49	2.72	3.02	2.52	2.54	1.18	1.22	1.41	1.23	1.20	1.23	2.77
Slope, S (°)		2.76	1.69	1.71	6.24	1.39	1.36	0.59	0.59	1.33	0.69	0.82	0.87	1.46
No. Basins	4th order-subbasins	5	2	5	3	2	3	3	2	6	2	2	2	2
Area, mean (km²)		2.33	1.87	2.31	1.31	0.83	0.88	0.83	1.90	3.62	1.33	1.50	2.60	2.34
Area, range (km²)		0.4-3.6	1.5-2.2	0.9-4.1	0.6-2.1	0.7-0.9	0.5-1.2	0.7-1.0	0.9-2.8	0.9-4.9	0.7-1.9	1.4-1.6	1.2-3.9	2.1-2.5
Tot stream length (km)		110.17	39.25	99.43	36.78	12.87	23.35	30.38	43.87	163.30	26.21	32.93	57.28	40.95
Drainage density, mean (km/km²)		9.45	10.57	8.45	9.11	7.81	8.42	12.05	12.42	11.05	9.96	10.97	11.26	8.76
Drainage density, S (km/km²)		0.60	0.59	0.63	0.62	0.71	1.74	0.96	2.39	1.08	0.22	0.99	0.61	0.06
Hypsometric Integral, min		0.22	0.68	0.33	0.37	0.64	0.47	0.42	0.47	0.27	0.27	0.45	0.62	0.35
Hypsometric Integral, max		0.74	0.70	0.68	0.56	0.65	0.61	0.56	0.54	0.64	0.56	0.50	0.77	0.46
Hypsometric Integral, mean		0.38	0.69	0.46	0.41	0.64	0.59	0.50	0.52	0.35	0.54	0.47	0.66	0.39
Hypsometric Integral, S		0.18	0.01	0.11	0.07	0.00	0.05	0.06	0.03	0.11	0.02	0.03	0.06	0.06
Relief, mean (m)		45.67	54.50	66.20	40.50	38.50	46.00	16.00	25.00	47.00	21.00	16.00	24.50	59.50
Relief, S (m)		10.01	0.71	24.00	6.36	0.71	10.44	1.00	7.07	27.22	7.07	2.83	7.78	21.92
Slope, mean (°)		2.52	2.13	2.62	2.82	2.33	2.32	1.11	1.11	1.50	1.14	0.91	1.03	2.84
Slope, S (°)		1.17	0.23	0.65	1.16	0.19	0.70	0.07	0.09	0.61	0.06	0.03	0.06	0.21
No. Basins	3rd order-subbasins	29	6	21	10	4	9	9	11	27	7	12	7	7
Area, mean (km²)		0.54	0.26	0.41	0.26	0.32	0.38	0.36	0.34	0.40	0.29	0.36	0.27	0.55
Area, range (km²)		0.1-1.7	0.1-0.4	0.1-1.7	0.1-0.7	0.1-0.5	0.1-0.8	0.1-1.5	0.1-0.9	0.1-1.5	0.1-0.64	0.1-1.15	0.1-0.5	0.2-1.0
Tot stream length (km)		83.95	8.17	98.99	26.40	15.54	16.13	36.22	31.69	126.55	43.30	66.86	46.94	30.95
Drainage density, mean (km/km²)		10.00	12.65	8.98	9.27	7.93	9.03	11.17	11.11	10.07	9.94	10.22	11.52	10.75
Drainage density, S (km/km²)		2.22	4.36	3.04	2.06	1.37	2.96	3.39	2.00	1.94	2.34	2.02	4.37	2.08
Hypsometric Integral, min		0.18	0.43	0.36	0.32	0.63	0.33	0.36	0.44	0.30	0.50	0.32	0.43	0.35
Hypsometric Integral, max		0.72	0.59	0.65	0.57	0.71	0.77	0.72	0.73	0.73	0.69	0.81	0.77	0.58
Hypsometric Integral, mean		0.54	0.49	0.52	0.45	0.66	0.62	0.52	0.54	0.47	0.55	0.57	0.58	0.47
Hypsometric Integral, S		0.14	0.07	0.09	0.08	0.03	0.10	0.09	0.06	0.11	0.04	0.11	0.10	0.07
Relief, mean (m)		19.70	14.75	42.33	31.30	34.75	22.11	11.89	12.56	18.65	15.29	13.67	12.75	40.67
Relief, S (m)		6.85	10.31	23.09	12.05	3.50	11.45	3.66	2.92	14.03	7.85	5.88	3.2	16.31
Slope, mean (°)		2.42	1.92	2.93	2.90	2.17	1.85	1.07	1.27	1.32	1.13	1.05	0.92	2.85
Slope, S (°)		2.00	1.73	0.96	1.35	0.21	0.80	0.22	0.21	0.43	0.20	0.27	0.14	0.36
Uplift, mean (m)		**-9**	**2**	**-2**	**-1**	**0**	**4**	**-2**	**-3**	**-8**	**-6**	**-5**	**-4**	**28**
Uplift, S (m)		**10.97**	**2.52**	**1.56**	**4.76**	**0.02**	**2.87**	**1.70**	**2.62**	**3.75**	**3.18**	**3.79**	**2.82**	**23.25**
Uplift, max (m)		**6**	**8**	**8**	**12**	**0.6**	**8**	**2**	**2**	**10**	**0**	**2**	**1**	**60**

Table 2 continue

uplift index, and (2) that correlations between the morphometric variables characterizing the basin geometry are scale dependent relative to both, the dimension of the investigated basin area and the basin order.

5.3. Spatial variation in morphometric properties

In this section, selected geomorphic variables are examined, and the morphometrical properties of the 5th-order basins and their 4th-and 3rd-order subbasins are discussed. Because stream power, i.e., the ability of a drainage system to erode, depends on the dimension of drainage network (see stream gradient index results and correlation analysis), the investigated drainage basins were classified (Tab. 3) and compared with respect to their drainage area dimension (group 1: area <5 km^2; group 2: area = 5-10 km^2; group 3: area >10 km^2)

Basin area, basin relief and slope, drainage density. (Group 1: 7 small basins) 5th-order basins with uplift index values greater than 10 have remarkably smaller areas (2.6-2.7 km^2) and smaller total stream lengths (21-28.1 km) than basins with uplift indices <10 (3.88-4.54 km^2). On the other hand, drainage density does not show a direct correlation with these findings or with uplift index. Basin slope and relief are similar for all basins (2.06°-2.54° and 60-78, respectively) and does not show a correlation with the uplift index (Tab. 3). The data obtained from the 4th- and 3rd-order subbasins show a similar trend with the exception of basin slope which decreases with increasing uplift index. This relation remains to be interpreted.

(Group 2: 12 medium basins) Generally, the 5th-order basins with positive uplift indices have greater areas and smaller stream lengths than those with negative indices. Notably, the two basins with the greatest uplift index values (basins 1 and 29; Tab. 3) have small areas and small total stream lengths (4.76-4.91 and 35.02-36.69, respectively). Drainage density shows a decreasing trend with increasing uplift index. Basin relief tends to be high in basins with positive uplift index (85-129, with standard deviations 15.86 to 30.33), and small in those with negative values (47-64, with standard deviations 7.82 to 11.7). A significant correlation between the average basin slope and uplift index could not be recognized. 4th- and 3rd-order subbasins data support these findings.

(Group 3: 10 large basins) The differences between the basins of group 3 are very subtle and remarkable only in area and total stream length values. Basins with positive or slightly negative uplift indices (-2 to 9) are smaller (10.27-17.4 km^2) and have smaller total stream lengths (91.44-163.36 km) than basins with uplift indices <-2 (10.48-21.21 km^2 and 118.98-217.24 km). Drainage density, basin slope, and relief data could not be correlated with the uplift index (Tab. 3).

In a broader context, significant differences in drainage density, basin relief, and slope are visible between the 5th-order basins of the Thalbach, the Ill, the Largue, and the Bourbeuse rivers (Fig. 2 and Tab. 2). The 5th-order basins of the Ill, the Thalbach, and the Largue drainage areas, all of which share a common regional base level and have mostly positive uplift index mean and maxima (-9-14 and 0-32, respectively), show drainage densities between 7.7 and 10.59, reliefs ranging from 60 to 171, and slopes from 1.95° to 3.77°. Conversely, the Bourbeuse drainage area belonging to the Doubs river catchment area has smaller uplift index mean and maxima (-8 to -2 and 0-10, respectively), with the exception of basin 29 which is affected by tectonic folding (Fig. 2, Tab. 2). Accordingly, the Bourbeuse area (without basin 29) comprises greater drainage densities (10.48-11.44), smaller basin relief values (47 to 71) and smaller slope values (1.18° and 1.41°).

For the 7th-order drainage areas the left and right basin sides of the Ill and Largue rivers display an unequal spatial distribution of uplift index values (Fig. 5). In both cases the values of the right basin side are higher than the values on the left side (Fig. 5). This asymmetry is also observed for the 3rd-order basin areas where

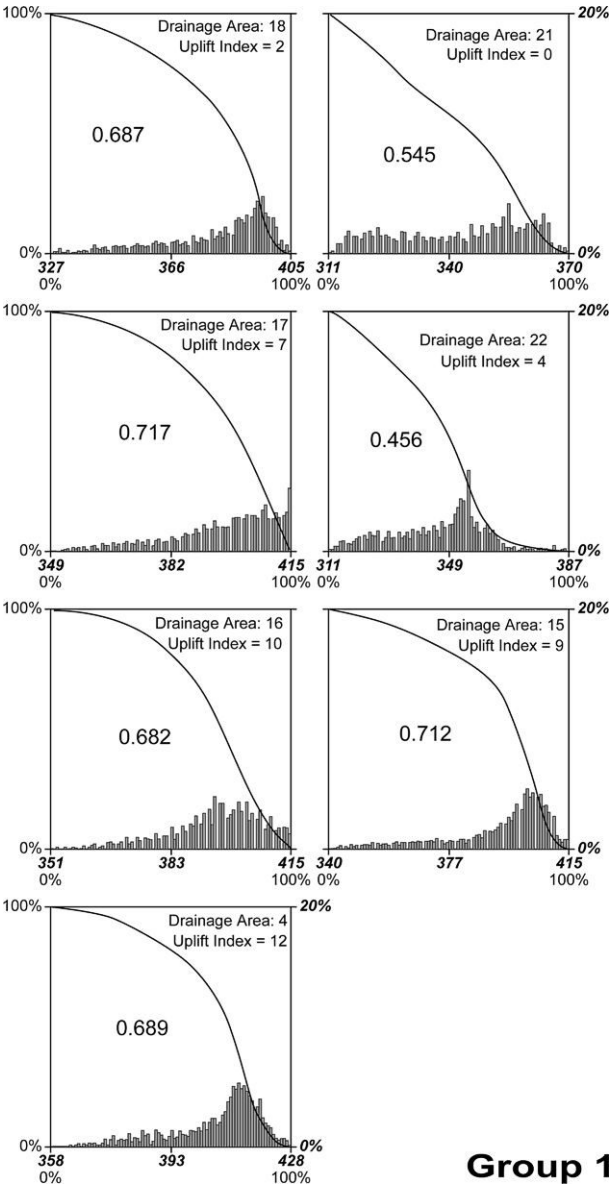

Figure 6a: Hypsometric curve and topographic distribution (columns) of 5th-order basins, Group1 (for grouping criteria see explanations in the text). For every basin the uplift index is given in the upper right.

the right basin side has a low number of relatively large subbasins and the left side has a larger number of relatively small subbasins. The asymmetry is less pronounced in the Thalbach drainage basin (Fig. 5).

Hypsometry. 23 out of 29 basins have hypsometric integral values between 0.5 and 0.72 (Tabs. 2, 3). The smallest values are around 0.3. Basins of group1 have integrals between 0.456 and 0.717, and 5 out of 7 basins show convex hypsometric curves with an asymmetric topographic distribution in the higher sectors (Fig. 6a-c). Only basins 21 (integral *I* = 0.54) and 22 (*I* = 0.45) have curves at the transition between convex and concave (Fig. 6a). Hypsometric data of the 5th-order basins as well as their 3rd- and 4th-order subbasins do not correlate with other morphometric parameters, nor does uplift index.

The integrals of the group 2-basins (Fig. 6b) with uplift indices <10 slightly increase with increasing uplift index value (*I* = 0.59-0.69). The integrals of basins with uplift indices >10 are very small (*I* = 0.31-0.35). This trend is also observed in 3rd- and 4th-order subbasins. Group2 hypsometric curves have a grater shape variety including convex curves (*I* = 0.66-0.69) with distribution in higher sectors (basins 28, 20, 14, 11), transitional curves (*I* = 0.54-0.63) with equal distribution or nearly normally distributed elevations (basins 26, 24, 23, 9, 7) and concave curves (I = 0.31-0.35) with elevations concentrated in the lower sectors.

Apart from basin 19 and 10, group 3-basins (Fig. 6c) have integrals between 0.5 and 0.64. Basins with integrals around 0.5 show s-shaped hypsometric curves with distributions concentrated in the middle segments. Basins with higher integrals have convex (*I* >0.6) or transitional (*I* = 0.53-0.55) curves and the distributions are shifted to the higher sectors (Fig. 6c). There is no evidence for a correlation between hypsometry and uplift index or other parameters.

Regionally a slight increase of average 4th-order hypsometric integrals from west to east, i.e., from the Bourbeuse area (*I* = 0.49) to the Largue (*I* = 0.53), the Ill (*I* = 0.57) and the Thalbach (*I* = 0.59) basins was observed (Tab. 2).

5.4. Discussion

In general, morphometric properties vary little throughout the study area. Therefore, the initial assumption of uniform climate and lithology is valid and tectonic activity, as recorded by the relief, is moderate. The presented results indicate that the topographic record of tectonic activity strongly depends on the spatial scale of the observed basins. Significant relationships between uplift index and geomorphic variables could only be observed for basins with areas between 5 and 10 km². The observed trends in drainage density and total stream length, together with the results of relief analysis (basin relief, hypsometry) can be explained as follows: Due to uplift, streams are rejuvenated, channels are downcut and stream gradients increase resulting in oversteepened reliefs. Larger drainage networks in basins > 10 km² are able to maintain their form through time by fast adjustment to lowering of the base level. Smaller basins with areas 5-10 km², however, are unable to incise an amount equal to

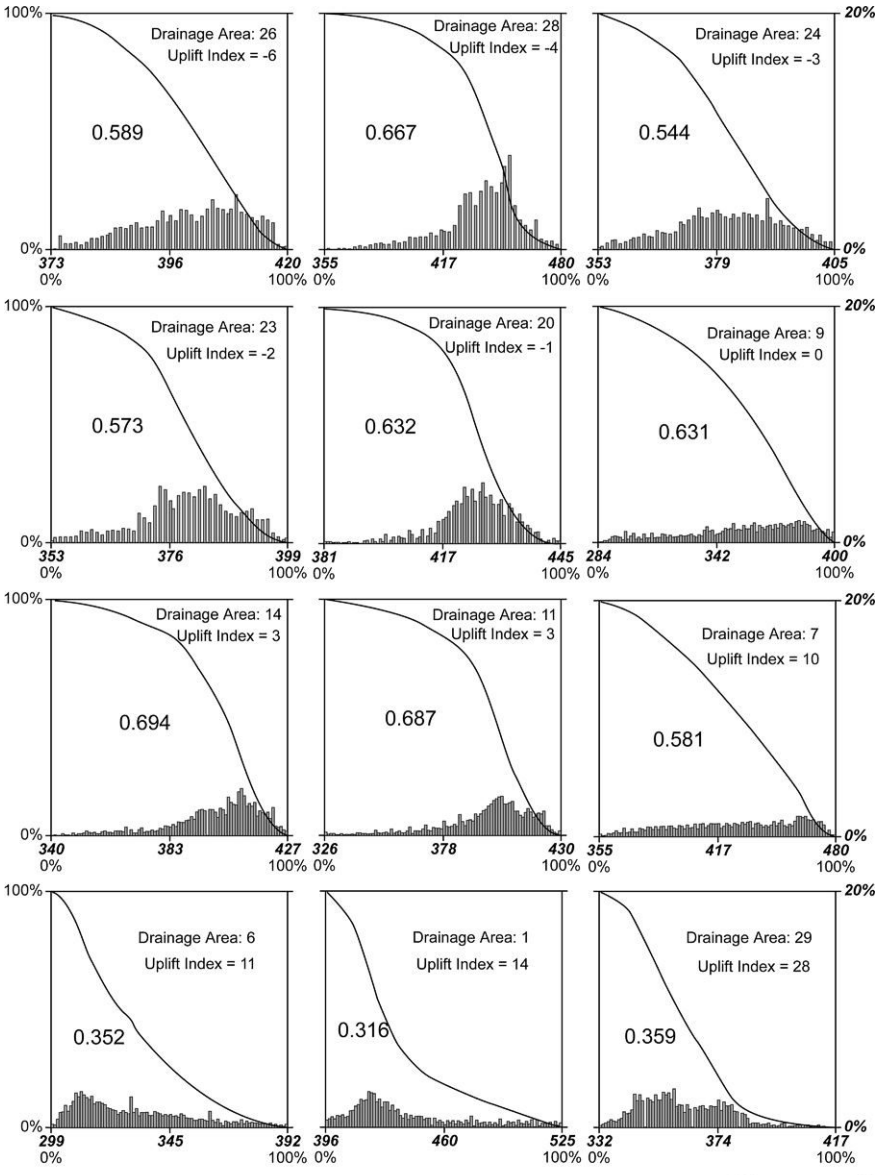

Figure 6b: Hypsometric curve and topographic distribution (columns) of 5th-order basins, Group2 (for grouping criteria see explanations in the text). For every basin the uplift index is given in the upper right.

the base-level fall. They therefore accumulate the effects of net base-level fall over a period of time. Their topographic response to tectonics is expressed through steep channel gradients in the area of highest uplift index (see section stream gradient index) and through increased erosion accompanied by subsequent merging of streams networks into single small branches (Giamboni et al., 2004b). With moderate uplift, drainage densities, relief, and, in part, hypsometric data show that the affected basins are drained by a small number of streams. Erosion occurs in the vertical scale (downcutting) producing a small drainage density, a moderate relief, and high hypsometric integrals (up to 0.7). At higher uplift rates, basins tend to be more elongated, smaller, and drained by streams with a lower total length. Relief index tends to be higher and the hypsometric integral to be small. The trends encountered in basins with higher uplift indices of group 3 match with results obtained in similar studies in more active areas (e.g. Merritts and Vincent, 1989; Ohmori, 1993; Willemin and Knuepfer, 1994; Hurtrez et al., 1999). Furthermore, hypsometric data imply that the classical subdivision of integral values (Strahler 1952) into inequilibrium (I = 0.6-1.0), equilibrium (I = 0.35-0.6), and areas of nearly flat surface (I <0.35) is not applicable in this case. On the contrary, areas with negative or moderate uplift index (<10), with some exceptions have large integrals between 0.5 and 0.7, and areas subject to active tectonics and higher uplift (uplift index >10) have smaller integrals between 0.2 and 0.5. This is compatible with the findings of Ohmori (1993) who states that young landscapes resulting from concurrent tectonics and denudation do not necessarily produce convex hypsometric curves, i.e., large integrals, but concave and/or s-shaped curves, i.e., moderate to small integrals.

Looking at drainage areas smaller than 5 km^2 the non significant correlation between basin properties and uplift index suggests that small basins are highly sensitive to local settings (noise), and variability can be related to spatial divergences on local climate and/or lithology changes. Conversely, by decreasing stream order, 3rd and 4th order basins broadly follow the trends observed in basins of 5th-order, even if they have a much smaller size, although correlations are generally decreasing and variability increases by decreasing order.

On a more regional scale, morphometric differences between the major drainage basins reflect the intricate morphological history of the study area. The capture of the westward draining Paleo-river to become the present-day Rhine River (Liniger, 1967; Petit et al., 1996; Villinger, 1998) led to the deviation of the Thalbach, the Ill, and the Largue drai nage systems. While their erosion base level fell significantly, the base level of the Bourbeuse system, still flowing to the west, remained basically un changed (Giamboni et al., 2004b). This explains the generally higher basin relief and slope index values of the eastern basins and their greater variability. However, the eastern basins are also subject to a greater uplift index leading to the superimposition of the topographic response to tectonism as shown by the base of the Sundgau gravel (Fig. 2).

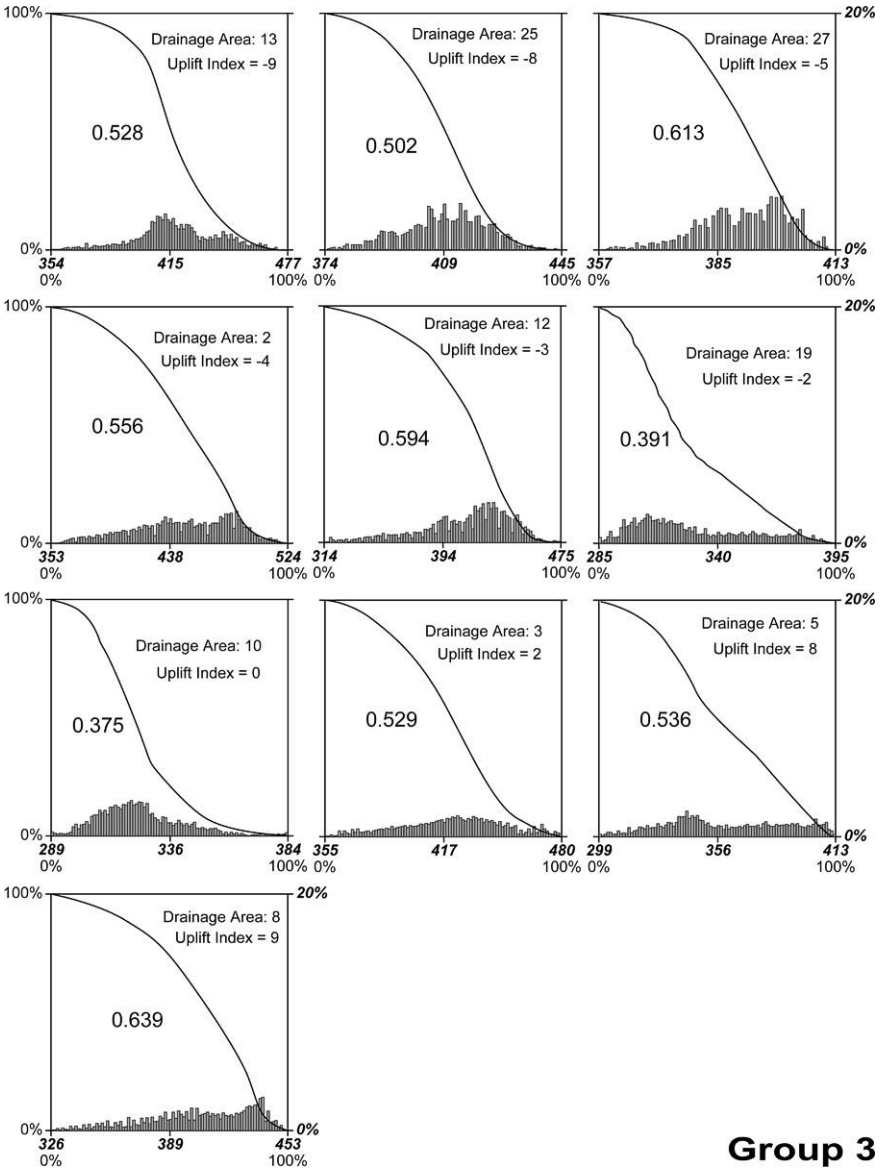

Figure 6c: Hypsometric curve and topographic distribution (columns) of 5th-order basins, Group3 (for grouping criteria see explanations in the text). For every basin the uplift index is given in the upper right.

6. Conclusions

Related to a marker horizon of Pliocene age, tectonic uplift areas were delineated and uplift indices were determined. Because lithology and

			5th order						4th order						3th order					
	ID	UI	Area	Stream	Dd	Hi	Relief	Slope	Area	Stream	Dd	Hi	Relief	Slope	Area	Stream	Dd	Hi	Relief	Slope
Group 1	21	0.00	3.88	31.96	8.24	0.54	60.00	2.52	0.83	12.87	7.81	0.64	38.50	2.33	0.32	15.54	7.93	0.66	34.75	2.17
	18	2.51	4.54	45.72	10.06	0.69	78.00	2.49	1.87	39.25	10.57	0.69	54.50	2.13	0.26	8.17	12.65	0.49	14.75	1.92
	22	4.35	4.27	36.64	8.58	0.46	76.00	2.54	0.88	23.35	8.42	0.59	46.00	2.32	0.38	16.13	9.03	0.62	22.11	1.85
	17	7.56	4.09	42.83	10.48	0.72	66.00	2.06	1.81	39.09	11.01	0.71	51.50	1.84	0.40	32.75	10.05	0.69	29.00	1.56
	15	9.51	4.46	45.66	10.23	0.71	75.00	2.46	1.13	24.52	10.85	0.72	43.50	1.93	0.18	30.94	10.20	0.66	32.50	1.89
	16	10.26	2.66	28.17	10.59	0.68	64.00	2.22	0.63	15.43	12.26	0.55	21.00	1.41	0.35	13.05	10.27	0.61	19.00	1.70
	4	12.25	2.70	21.00	7.79	0.68	70.00	2.08	0.94	14.31	7.58	0.69	39.00	1.67	0.45	9.60	7.84	0.58	15.40	1.49
			5th order						4th order						3th order					
	ID	UI	Area	Stream	Dd	Hi	Relief	Slope	Area	Stream	Dd	Hi	Relief	Slope	Area	Stream	Dd	Hi	Relief	Slope
Group 2	26	-6.39	6.86	72.75	10.61	0.59	47.00	1.23	1.33	26.21	9.96	0.54	21.00	1.14	0.29	43.30	9.94	0.55	15.29	1.13
	28	-4.25	6.58	68.95	10.48	0.68	47.00	1.23	2.60	57.28	11.26	0.66	24.50	1.03	0.27	46.94	11.52	0.58	12.75	0.92
	24	-2.63	6.34	71.69	11.31	0.55	52.00	1.22	1.90	43.87	12.42	0.52	25.00	1.11	0.34	31.69	11.11	0.54	12.56	1.27
	23	-1.98	5.53	63.22	11.44	0.57	47.00	1.18	0.83	30.38	12.05	0.50	16.00	1.11	0.36	36.22	11.17	0.52	11.89	1.07
	20	-1.28	5.77	56.81	9.85	0.63	64.00	3.02	1.31	36.78	9.11	0.41	40.50	2.82	0.26	26.40	9.27	0.45	31.30	2.90
	9	0.07	7.07	64.37	9.10	0.64	116.00	3.77	1.85	50.01	8.32	0.67	86.33	3.63	0.49	33.36	9.37	0.65	54.55	3.59
	14	2.83	6.88	68.38	9.93	0.69	88.00	2.21	1.87	58.82	9.96	0.71	48.00	1.98	0.37	34.08	10.35	0.62	15.80	1.45
	11	3.06	5.73	52.96	9.25	0.69	104.00	1.95	1.80	36.76	10.22	0.63	53.50	1.56	0.38	17.29	10.45	0.66	16.40	1.25
	7	10.32	7.14	65.49	9.18	0.59	120.00	2.66	1.72	45.38	8.85	0.64	81.67	2.38	0.23	29.73	9.33	0.62	42.11	2.21
	6	11.00	7.93	69.82	8.80	0.35	94.00	2.77	0.95	34.15	9.19	0.37	67.25	3.03	0.31	34.99	10.24	0.44	49.70	2.82
	1	14.27	4.76	36.69	7.70	0.31	129.00	2.85	2.15	31.89	7.41	0.43	86.50	2.99	0.79	26.80	6.66	0.42	67.33	3.10
	29	27.89	4.91	35.02	7.13	0.35	85.00	2.77	2.34	40.95	8.76	0.39	59.50	2.84	0.55	30.95	10.75	0.47	40.67	2.85
			5th order						4th order						3th order					
	ID	UI	Area	Stream	Dd	Hi	Relief	Slope	Area	Stream	Dd	Hi	Relief	Slope	Area	Stream	Dd	Hi	Relief	Slope
Group 3	13	-9.57	20.80	196.04	9.42	0.53	128.00	2.66	2.33	110.17	9.45	0.38	45.67	2.52	0.54	83.95	10.00	0.54	19.70	2.42
	25	-7.90	19.76	217.24	11.00	0.50	71.00	1.41	3.62	163.30	11.05	0.35	47.00	1.50	0.40	126.55	10.07	0.47	18.65	1.32
	27	-5.46	10.48	118.98	11.36	0.63	56.00	1.20	1.50	32.93	10.97	0.47	16.00	0.91	0.36	66.86	10.22	0.57	13.67	1.05
	2	-4.18	20.34	158.31	7.78	0.56	171.00	2.88	3.22	88.40	9.04	0.55	66.33	1.50	0.31	62.44	10.34	0.59	42.53	2.55
	12	-2.80	21.21	204.06	9.62	0.59	162.00	3.11	2.13	129.29	10.42	0.41	52.25	2.23	0.52	87.47	11.82	0.50	24.22	2.55
	19	-1.96	16.49	141.53	8.59	0.40	110.00	2.72	2.31	99.43	8.45	0.46	66.20	2.62	0.41	98.99	8.98	0.52	42.33	2.93
	10	-0.05	10.27	91.44	8.90	0.38	95.00	3.40	2.48	61.53	8.76	0.42	67.33	3.84	0.52	52.00	10.13	0.45	56.18	4.16
	3	2.36	15.40	149.02	9.68	0.53	126.00	2.38	4.61	82.84	8.79	0.56	84.50	2.04	0.51	82.46	10.45	0.63	50.79	2.20
	5	8.36	17.40	163.36	9.39	0.54	115.00	2.42	2.72	98.03	9.35	0.59	58.50	1.95	0.40	85.10	8.90	0.56	38.57	2.25
	8	8.87	11.97	106.65	8.91	0.64	127.00	2.34	0.90	32.92	9.02	0.53	24.75	1.11	0.44	44.23	10.28	0.57	17.92	1.18

Table 2 continue: Morphometric properties of 5th-order basins and their 4th- and 3rd-order subbasins (average values), grouped by area dimension (for grouping criteria see explanations in the text).

climate do not vary considerably, it is assumed that tectonic uplift is the dominant variable for erosional processes. An extensive number of morphometric properties of drainage basins were used to investigate if spatial variations of uplift have effected the drainage evolution and the alluvial dynamics, and, therefore, if tectonism is ongoing.

(1) The small amount of variation of the morphometric properties throughout the study area implies uniform climatic and lithological conditions and moderate tectonic activity.

(2) Morphometric parameters related to channel network properties (drainage density, total stream length) and to channel beds (stream gradient index) significantly correlate to tectonic uplift. Stream gradient analysis provided the best results for identifying the processes affecting the present-day alluvial rivers (e.g., tectonic uplift, lithology changes): The primary responses to uplift are incision and channel steepening due to base-level fall and physical tilting. Geomorphic properties related to the drainage basin geometry (basin relief, slope, and hypsometry) are only in part associated to tectonic effects, and probably obeys some laws, that are independent of uplift, climate and lithology.

(3) The hypsometry shows the reverse trend from the classical Strahler's interpretation.

(4) The topographic record of tectonic activity is strongly depending on the spatial scale of the observed basins. The most significant relationships between uplift index and selected geomorphic variables have been recognized in basins with areas ranging from 5 to 10 km². Basins with larger areas could already adjust to the base level change, while the geomorphic response of small basins (<5 km²) is perturbed by local diversity and noise.

Although correlation between tectonic and geomorphic variables decreases with decreasing Horton order, the average values of 3rd- and 4th-order subbasins reflect the general trend of their 5th-order basin.

(5) Regional differences on base level between the Rhinegraben (Ill catchment area) and the Bressegraben (Doubs catchment area) are only visible when comparing the properties of 7th-order drainage basins.

(6) Morphometric analysis provides evidences for ongoing tectonic activity in the southern Rhinegraben, as also shown by geodetic surveys in the southern Rhinegraben (Liaghat et al., 1998) and geological investigations on the Quaternary of the Rhine River Valley between Schaffhausen and Basel (e.g. Verderber, 2003; Müller et al., 2002).

The methods presented have been tested in regions where climate and rock resistances are uniform and uplift rates are high and well constrained. Nonetheless, this study demonstrates that they provide useful tools to evidence active tectonism, even in regions of slow tectonic deformation as the southern Rhinegraben.

Acknowledgement

The authors thank the Fachhochschule Beider Basel (FHBB) and especially R. Stibler for providing leveling instruments. The manuscript substantially benefited from thorough and constructive reviews by two anonymous reviewer

References

Bull, W.B. 1990. Stream-terrace genesis: implications for soil development. Geomorphology, 3, 351-367.

Bull, W.L. and Knuepfer, P.L.K. 1987. Adjustments by the Charwell River, New Zealand, to uplift and climatic changes. Geomorphology, 1, 15-32.

Contini, D., Kuntz, G., Angély, B., Laffly, J.L., Kerrien, Y., Landry, J. and Théobald, N. 1973. Carte Géologique et Notice Explicative, Feuille 3522 Montbéliard. BRGM, Orleans.

Doebl, F. 1970. Die tertiären und quartären Sedimente des südlichen Rheingraben. In: J.H. Illies and S. Mueller (Editors), Graben Problems. Schweizerbart, Stuttgart, pp. 56-66.

Galay, V.J. 1983. Causes of river bed degradation. Water Resources Research, 19, 1057-1090.

Giamboni, M., Ustaszewski, K., Schmid, S.M., Schumacher, M. and Wetzel, A. 2004 (a). Plio-Pleistocene transpressional reactivation of Paleozoic and Paleogene structures in the Rhine-Bresse Transform Zone (Northern Switzerland and Eastern France). International Journal of Earth Sciences, 93, 207-223.

Giamboni, M., Wetzel, A., Nivière, B. and Schumacher, M. 2004 (b). Plio-Pleistocene folding in the southern Rhinegraben recorded by the evolution of the drainage network (Sundgau area; northwestern Switzerland and France). Eclogae geologicae Helvetiae 97(2004), 17-31.

Gilbert, G.K., 1877. Report on the Geology of the Henry Mountains. U.S. Geographical and Geological Survey, Washington, 160 pp.

Hack, J.T. 1957. Studies of longitudinal stream profiles in Virginia and Maryland. U. S. Geolological Survey Professional Papers, 294-B, 97.

Hack, J.T. 1973. Stream-profile analysis and stream-gradient index. Journal of Research U. S. Geolological Survey, 1(4), 421-429.

Horton, R.E. 1932. Drainage basin characteristics. Transactions of the American Geophysical Union, 14, 350-361.

Horton, R.E. 1945. Erosional development of streams and their drainage basisn; hydrophysical approach to quantitative morphology. Bulletin of the Geological Society of America, 56, 275-370.

Hurtrez, J.E., Lucazeau, F., Lavé, J. and Avouac, J.-P. 1999. Investigation of the relationship between basin morphology, tectonic uplift, and denudation from the study of an active fold belt in the Siwalik Hills, central Nepal. Journal of Geophysical Research, 104(B6), 12779-12796.

Keller, E.A. 1986. Investigations of active tectonics: use of surficial earth processes. In: R.E. Wallace (Editor), Active Tectonics. National Academy Press, Washington DC, pp. 136-147.

Keller, E.A. and Pinter, N. 2002. Active Tectonics: Earthquakes, Uplift and Landscape. Prentice Hall, Upper Saddle River, 362 pp.

Laubscher, H. 2001. Plate interactions at the southern end of the Rhine graben. Tectonophysics, 343, 1-19.

Liaghat, C., Villemin, T. and Jouanne, F. 1998. Déformation verticale actuelle dans la partie sud du fossé d'Alsace (France). Earth & Planetary Sciences 327, 55-60.

Lifton, N.A. and Chase, C.G. 1992. Tectonic, climatic and lithologic influences on landscape fractal dimension and hypsometry: implications for landscape evolution in the San Gabriel Mountains, California. Geomorphology, 5, 77-114.

Liniger, H. 1966. Das plio-altpleistozäne Flussnetz der Nord-schweiz. Regio Basiliensis, 7(2), 158-177.

Liniger, H. 1967. Pliozän und Tektonik des Juragebirges. Eclogae geolocicae Helvetiae, 60(2), 407-490.

Mackin, J.H. 1948. Concept of the graded stream. Bulletin of the Geological Society of America, 59, 463-512.

McKeown, F.A., Jones-Cecil, M., Askew, B.L. and McGrath, M.B. 1988. Analysis of stream-profile data and inferred tectonic activity, eastern Ozark Mountains region. U. S. Geological Survey Bulletin, 1807, 1-39.

Meghraoui, M., Delouis, B., Ferry, M., Giardini, D., Huggenberger, P., Spottke, I. and Granet, M. 2001. Active normal faulting in the Upper Rhine Graben and paleoseismic identification of the 1356 Basel earthquake. Science, 293, 2070-2073.

Ménillet, F., Coulon, M., Fourquin, C., Paicheler, J.-C., Lougnon, J.-M. and Lettermann, M. 1989. Carte Géologique et Notice Explicative, Feuille 3620 Thann. BRGM, Orleans.

Merritts, D.J. and Vincent, K.R. 1989. Geomorphic response of coastal streams to low, intermediate, and high rates of uplift, Mendocino triple junction region, northern California. Bulletin of the Geological Society of America, 101, 1373-1388.

Merritts, D.J., Vincent, K.R. and Wohl, E.E. 1994. Long river profiles, tectonism, and eustasy: A guide to interpreting fluvial terraces. Journal of Geophysical Research, 99(B7), 14031-14050.

Müller, W.H., Naef, H. and Graf, H.R. 2001. Zur Tektonik der zentralen Nordschweiz - Interpretation aufgrund regionaler Seismik, Oberflächengeologie und Tiefbohrugen. Nagra Technischer Bericht NTB 99-08, Nagra, Wettingen, 226 pp.

Müller, W.H., Naef, H. and Graf, H.R., 2002. Geologische Entwicklung der Nordschweiz, Neotektonik und Langzeit-szenarien Zürcher Weinland. NAGRA Technischer Bericht, 99-08. NAGRA, Wettingen, 237 pp.

Nivière, B. and Winter, T. 2000. Pleistocene nothwards fold propagation of the Jura within the southern Upper Rhine Graben: Seismotectonic implications. Global and Planetary Change, 27, 263-288.

Ohmori, H. 1993. Changes in the hypsometric curve through mountain building resulting from concurrent tectonics and denudation. Geomorphology, 8, 263-277.

Ouchi, S. 1985. Response of alluvial rivers to slow active tectonic movement. Bulletin of the Geological Society of America, 96, 504-515.

Petit, C., Campy, M., Chaline, J. and Bonvalot, J. 1996. Major palaeohydrographic changes in Alpine foreland during the Pliocene-Pleistocene. Boreas, 25, 131-143.

Ruhland, M. and Blanat, J.G. 1973. Carte Géologique et Notice Explicative, Feuille 3722 Ferrette. BRGM, Orleans.

Schumacher, M. 2002. Upper Rhine Graben: Role of preexisting structures during rift evolution. Tectonics, 21(1), 6.1 – 6.17.

Schumm, A.S. 1981. Evolution and response of the fluvial system, sedimentologic implications. International Association of Sedimentology Special Publication, 31, 19-39.

Schumm, S.A. 1986. Alluvial river response to active tectonics. In: N.R. Council (Editor), Active Tectonics. National Academy Press, Washington (D.C.), pp. 80-94.

Schumm, S.A. 1993. River response to baselevel change: implications for sequence stratigraphy. Journal of Geology, 101, 279-294.

Seeber, L. and Gornitz, V. 1983. River profiles along the Himalayan arc as indicators of active tectonics. Tectonophysics, 92, 335-367.

Sissingh, W. 1998. Comparative Tertiary stratigraphy of the Rhine Graben, Bresse Graben and Molasse Basin: correlation of Alpine foreland events. Tectonophysics, 300, 249-284.

Strahler, A.N. 1952. Hypsometric (area-altitude) analysis of erosional topography. Bulletin of the Geological Society of America, 63, 1117-1142.

Summerfield, M.A. and Hulton, N.J. 1994. Natural controls of fluvial denudation rates in major world drainage basins. Journal of Geophysical Research, 99(B7), 13871-13883.

Théobald, N. and Devantoy, J. 1963. Carte Géologique et Notice Explicative, Feuille 3621 Belfort. BRGM, Orleans.

Théobald, N. and Dubois, G. 1958. Carte Géologique et Notice Explicative, Feuille 3721 Altkirch-Huningue. BRGM, Orleans.

Ustaszewski, K., Schmid, S.M. and Giamboni, M. 2001. The frontal folds of the Jura mountains revisited: subsequent folding of Oligocene extensional structures during a thick-skinned phase of Jura folding? Journal of Conference Abstracts, 6(1), 630.

Verderber, R. 2003. Quartärgeologie im Hochrheingebiet zwischen Schaffhausen und Basel. Zeitschrift der deutschen geologischen Gesellschaft 154, 369-406.

Vergnes, M. and Souriau, M. 1993. Quantifying the transition between tectonic trend and mesoscale texture in topographic data. Geophysical Research Letters, 20, 2139-2141.

Villinger, E. 1998. Zur Flussgeschichte von Rhein und Donau in Südwestdeutschland. Jahrbuch der oberrheinischen geologischen Vereinigung, 80, 361-398.

Willemin, J.H. and Knuepfer, L.K. (1994). Kinematics of arc-continent collision in the eastern Central Range of Taiwan inferred from geomorphic analysis. Journal of Geophysical Research, 99(B10), 20.267-20.280.

Zuchiewicz, W. 1995. Time-series analysis of river bed gradients in the Polish Carpathians: a statistical approach to the studies on young tectonic activity. Zeitschrift für Geomorphologie Neue Folge, 39(4), 461-477.

Received: 9. June 2004
Accepted: 8. June 2005

M. GIAMBONI*), A. WETZEL & B. SCHNEIDER

Geologisch-Paläontologisches Institut, Universität Basel, Bernoullistrasse 32, CH-4055 Basel

*) coresponding author (present address): Forstdirektion - Schutzwald und Naturgefahren Bundesamt für Umwelt, Wald und Landschaft CH-3003 Bern